

## Electronic Supporting Information

### Imidazopyridine-Fluoride Interaction: Solvent-switched AIE Effect via S...O Conformational Locking

Annu Kumari<sup>a</sup>, Wim Dehaen<sup>b</sup>, Deepak Chopra<sup>\*c</sup>, and Swapan Dey<sup>\*a</sup>

<sup>a</sup>Department of Chemistry and Chemical Biology, Indian Institute of Technology (ISM), Dhanbad 826004, India. Email: [swapan@iitism.ac.in](mailto:swapan@iitism.ac.in)

<sup>b</sup>Molecular Design & Synthesis, Department of Chemistry, KU Leuven, Celestijnenlaan 200F, B-3001 Leuven, Belgium

<sup>c</sup>Crystallography & Crystal Chemistry Laboratory, Department of Chemistry, IISER Bhopal, 462066, India. Email: [dchopra@iiserb.ac.in](mailto:dchopra@iiserb.ac.in)

Table of Contents:	Page
1. Crystal data of C1, C2, C1.S and C2.S and H-bonding data	2-3
2. Spectroscopic characterization of compounds	4-8
3. LOD, binding constant, and stoichiometry	8-10
4. Emission titration	10-11
5. The peculiar behavior of C1 in CHCl <sub>3</sub>	11
6. D <sub>2</sub> O exchange of compounds in <sup>1</sup> H NMR	12-13
7. <sup>1</sup> H and <sup>19</sup> F NMR spectra of complexes	14-15
8. FT-IR spectroscopy	16
9. HR-MS spectrum of complexes	16-17
10. DFT calculated optimized structure	18
11. Titration plot of carboxamide with CN <sup>-</sup>	18-19
12. FE-SEM image	20
13. References	20

## Crystal data of C1, C2, C1.S, and C2.S and H-bonding data

**Table S1. Crystal data**

Compound	C1	C2	C1.S	C2.S
CCDC No.	2085440	2085441	2085442	2085443
Empirical formula	C <sub>15</sub> H <sub>9</sub> ClN <sub>4</sub> O <sub>5</sub>	C <sub>15</sub> H <sub>10</sub> ClN <sub>5</sub> O	C <sub>31</sub> H <sub>48</sub> Cl N <sub>5</sub> O <sub>3</sub> S	C <sub>31</sub> H <sub>49</sub> Cl N <sub>6</sub> O <sub>3</sub>
Formula weight	328.77	311.73	606.25	589.21
Temperature/K	292(2)	292(2)	292(2)	292(2)
Crystal system	Monoclinic	Triclinic	Monoclinic	Orthorhombic
Space group	<i>P</i> 2 <sub>1</sub> / <i>c</i>	<i>P</i> -1	<i>P</i> 2/ <i>c</i>	<i>Pbcn</i>
a/Å	8.0687(8)	6.5832(8)	23.0412(9)	46.3890(18)
b/Å	6.5157(5)	7.6795(10)	9.3628(4)	9.2469(6)
c/Å	26.9123(17)	13.7007(13)	15.7390(7)	15.7793(9)
α/°	90	97.024(9)	90	90
β/°	90.204(7)	91.925(9)	98.319(4)	90
γ/°	90	96.046(10)	90	90
Volume/Å <sup>3</sup>	1414.9(2)	682.87(14)	3359.6(2)	6768.6(6)
Z	4	2	4	8
ρ <sub>calc</sub> /cm <sup>3</sup>	1.543	1.516	1.199	1.156
μ/mm <sup>-1</sup>	0.424	0.289	0.213	0.151
F(000)	672.0	320.0	1304.0	2544.0
Crystal size/mm <sup>3</sup>	0.13 × 0.12 × 0.11	0.068 × 0.056 × 0.044	0.056 × 0.045 × 0.033	0.150 × 0.140 × 0.110
Radiation	MoKα (λ = 0.71073)	MoKα (λ = 0.71073)	MoKα (λ = 0.71073)	MoKα (λ = 0.71073)
2θ range/°	6.056 to 57.86	5.378 to 50.992	5.076 to 57.802	4.492 to 58.792
Index ranges	-10 ≤ h ≤ 9, -8 ≤ k ≤ 7, -35 ≤ l ≤ 32	-7 ≤ h ≤ 7, -8 ≤ k ≤ 9, -16 ≤ l ≤ 16	-30 ≤ h ≤ 30, -10 ≤ k ≤ 12, -20 ≤ l ≤ 21	-63 ≤ h ≤ 59, -12 ≤ k ≤ 9, -17 ≤ l ≤ 21
Reflections collected	15957	4948	39938	22943
Independent reflections	3260 [R <sub>int</sub> = 0.0928]	2536 [R <sub>int</sub> = 0.0266]	7806 [R <sub>int</sub> = 0.0824]	8095 [R <sub>int</sub> = 0.066]
Data/restraints/parameters	3260/0/204	2536/0/207	7806/0/390	8095/50/407
Goodness-of-fit on F <sup>2</sup>	1.102	1.026	1.012	0.954
Final R indexes [I ≥ 2σ(I)]	R <sub>1</sub> = 0.0902, wR <sub>2</sub> = 0.2512	R <sub>1</sub> = 0.0530, wR <sub>2</sub> = 0.1037	R <sub>1</sub> = 0.0560, wR <sub>2</sub> = 0.1362	R <sub>1</sub> = 0.0653, wR <sub>2</sub> = 0.1336
Final R indexes [all data]	R <sub>1</sub> = 0.1044, wR <sub>2</sub> = 0.2578	R <sub>1</sub> = 0.1089, wR <sub>2</sub> = 0.1274	R <sub>1</sub> = 0.0925, wR <sub>2</sub> = 0.1523	R <sub>1</sub> = 0.2003, wR <sub>2</sub> = 0.1890
Largest diff. peak/hole / eÅ <sup>-3</sup>	0.55/-0.40	0.20/-0.24	0.24/-0.29	0.18/-0.28

**Table S2: H-bonding data**

Interactions	D-H	H...A (Å)	D...A (Å)	D-H...A (°)	Symmetry code
<b>C1</b>					
<b>N3-H3 ...N2</b>	0.97(8)	2.36(8)	2.744(8)	102(6)	x,y,z
<b>C1-H1 ...N2</b>	0.93	2.72	3.612(9)	162	-x+2,-y,-z+1
<b>C2-H2...N4</b>	0.93	2.86	3.735(10)	158	-x+2,-y,-z+1
<b>C12-H12...O1</b>	0.93	2.65	3.366(10)	134	-x+1,-y+2,-z+1
<b>C2</b>					
<b>N2-H2...O1</b>	0.83(3)	2.32(3)	2.810(3)	118(3)	x, y, z
<b>N2-H2 ...O1</b>	0.83(3)	2.46(3)	3.104(3)	136(3)	-x,-y+1,-z+1
<b>C13-H13 ...N1</b>	0.93	2.65	3.544(4)	162	-x+2,-y+2,-z+1
<b>C14-H14 ...N5</b>	0.93	2.71	3.610(4)	163	-x+2,-y+2,-z+1
<b>C1.S</b>					
<b>O2-H101...O3</b>	0.82(3)	2.02(3)	2.837(3)	176(3)	x, y, z
<b>O3-H102 ...N3</b>	0.86(3)	2.08(3)	2.909(3)	162(3)	x, y, z
<b>C12-H12...O2</b>	0.93	2.62	3.199(3)	121	-x+1,-y+1,-z+1
<b>O2-H100...N2</b>	0.83(3)	2.16	2.980(2)	169(3)	x,+y-1,+z
<b>O3-H103...N1</b>	0.81(3)	2.37(4)	3.071(2)	146(3)	x,+y-1,+z
<b>C2.S</b>					
<b>O2-H2A ...N3</b>	0.84(4)	2.17(4)	2.992(4)	166(4)	x, y, z
<b>O2-H2B...O3</b>	0.92(4)	1.98(4)	2.861(4)	160(4)	x, y, z
<b>O3-H3C ...N5</b>	0.83(4)	2.22(4)	2.925(4)	143(4)	x, y, z
<b>N4-H4 ...O1</b>	0.86	2.01	2.563(3)	121	x, y, z
<b>O3-H3B ...N2</b>	0.82(4)	2.16(4)	2.941(4)	162(4)	x,+y+1,+z
<b>C2-H2 ...O2</b>	0.93	2.64	3.240(5)	123	-x+1,-y+1,-z+2

## Spectroscopic characterization of compounds

Figure S1.  $^1\text{H}$ NMR (400MHz,  $\text{CDCl}_3$ ) of compound 1.

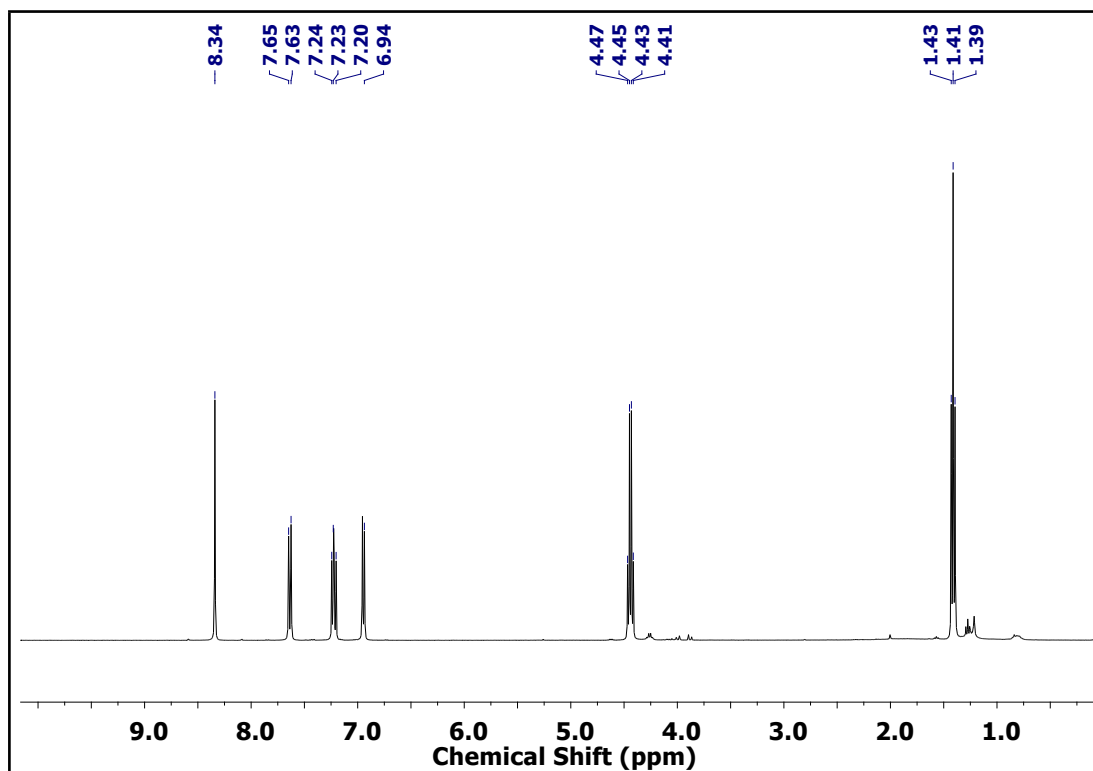


Figure S2.  $^{13}\text{C}$ NMR (100 MHz,  $\text{CDCl}_3$ ) of compound 1.

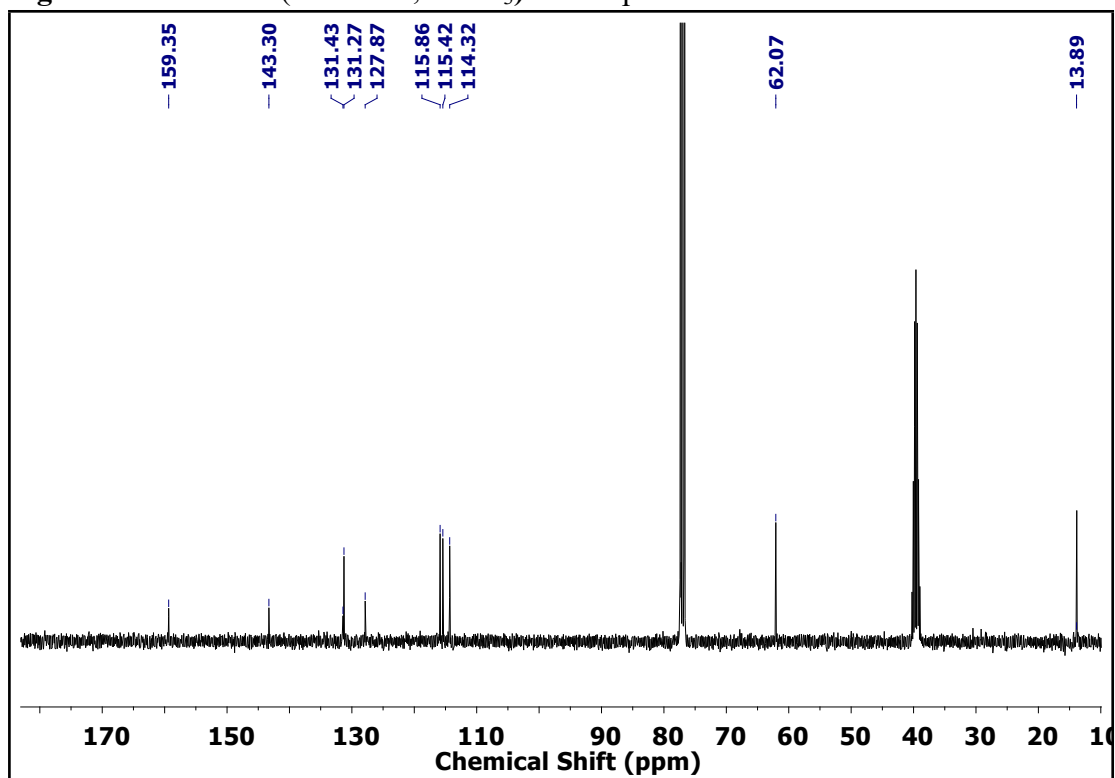


Figure S3.  $^1\text{H}$ NMR (400 MHz,  $d_6$ -DMSO) of compound C1.

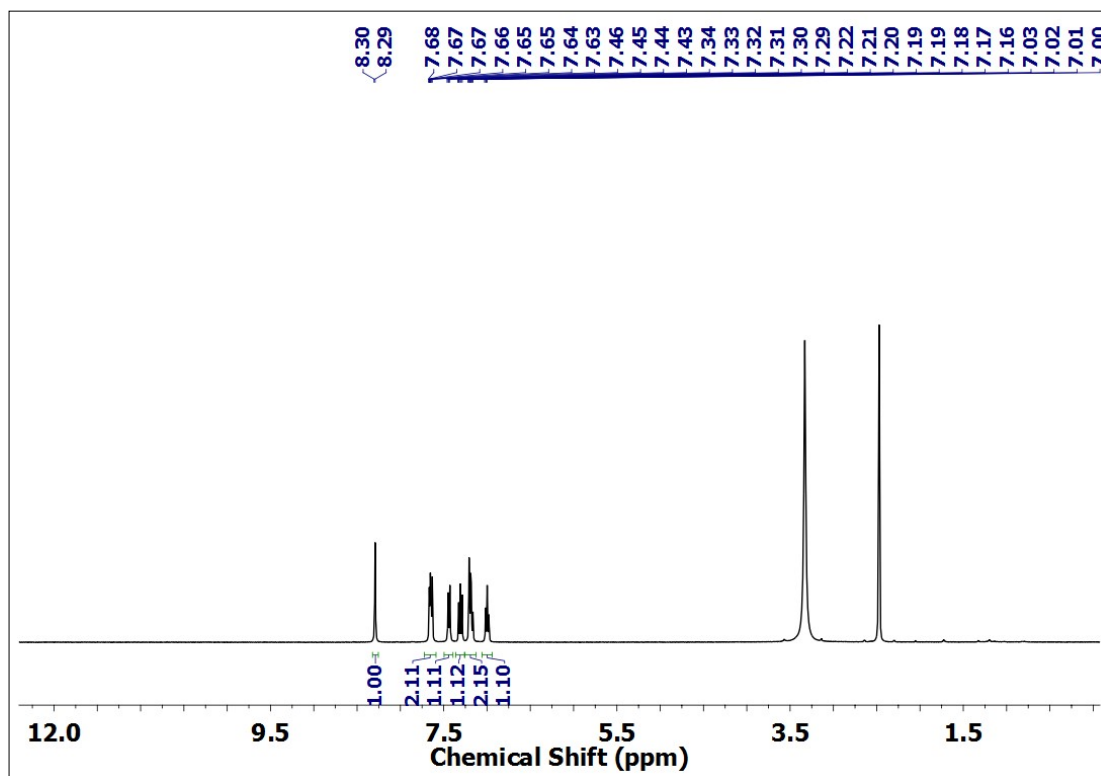


Figure S4.  $^{13}\text{C}$ NMR (100 MHz,  $d_6$ -DMSO) of compound C1.

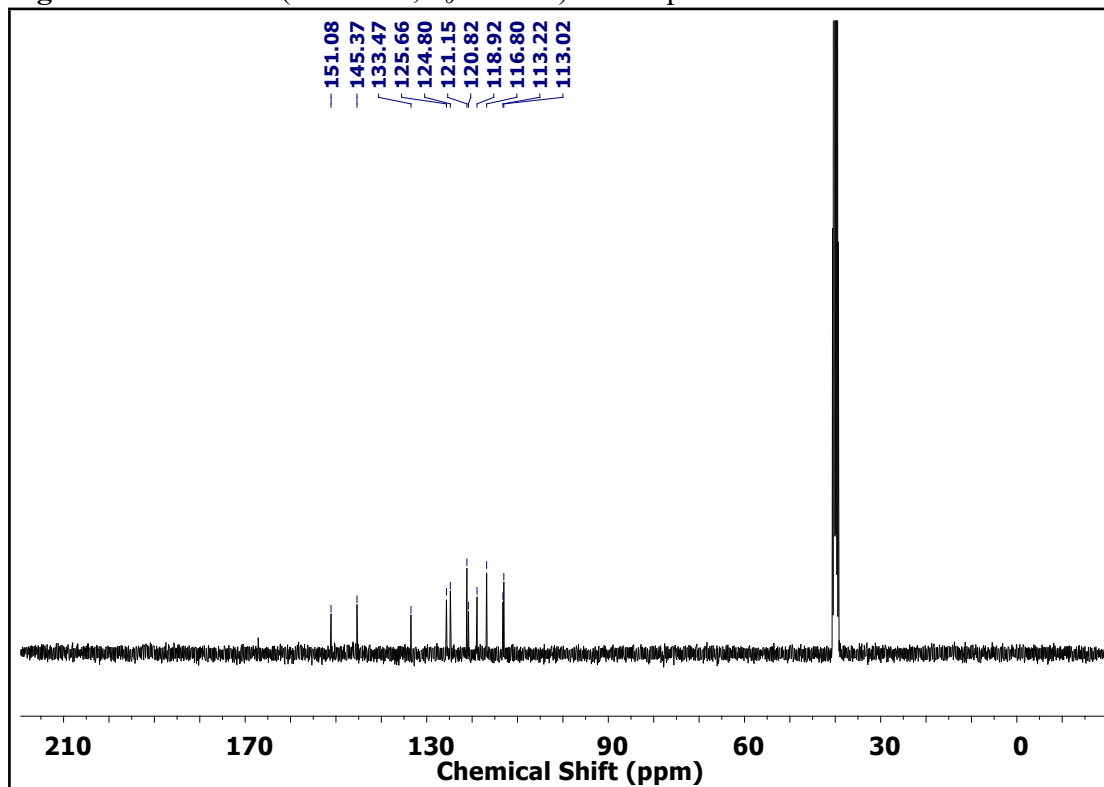


Figure S5.  $^1\text{H}$ NMR (400 MHz, DMSO) of compound C2.

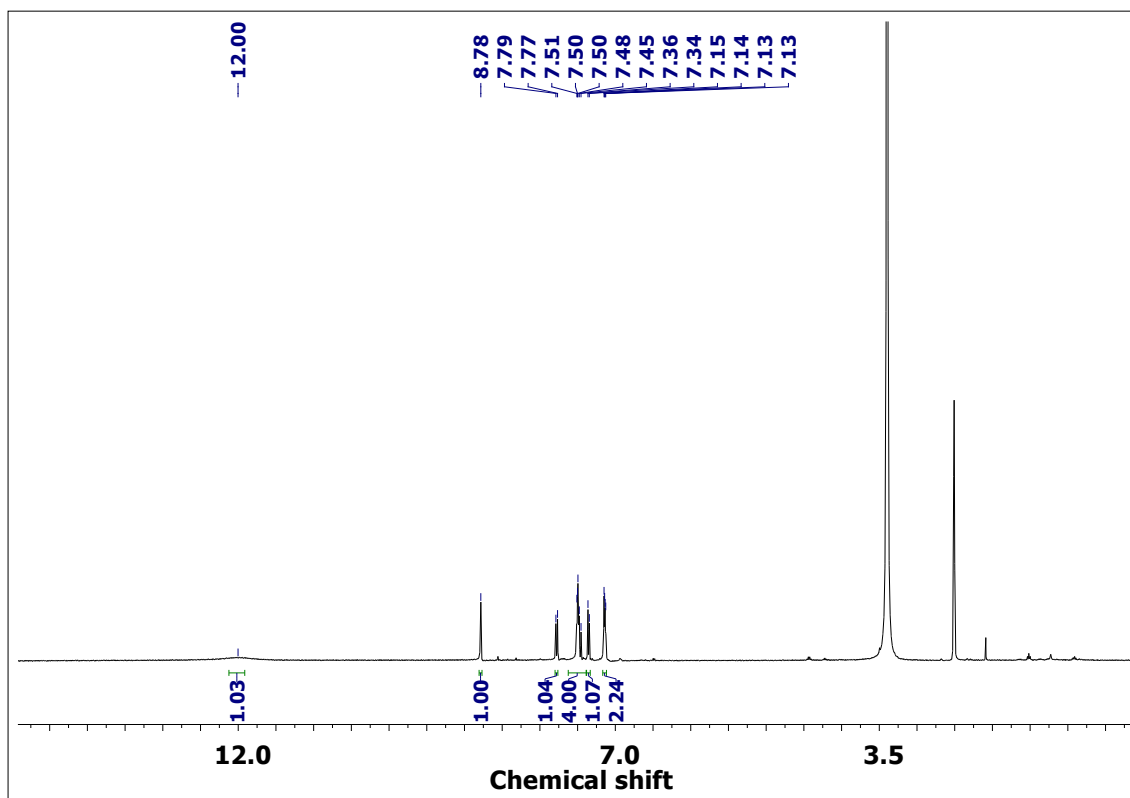


Figure S6.  $^1\text{H}$ NMR (400 MHz,  $\text{CDCl}_3$ ) of compound C2.

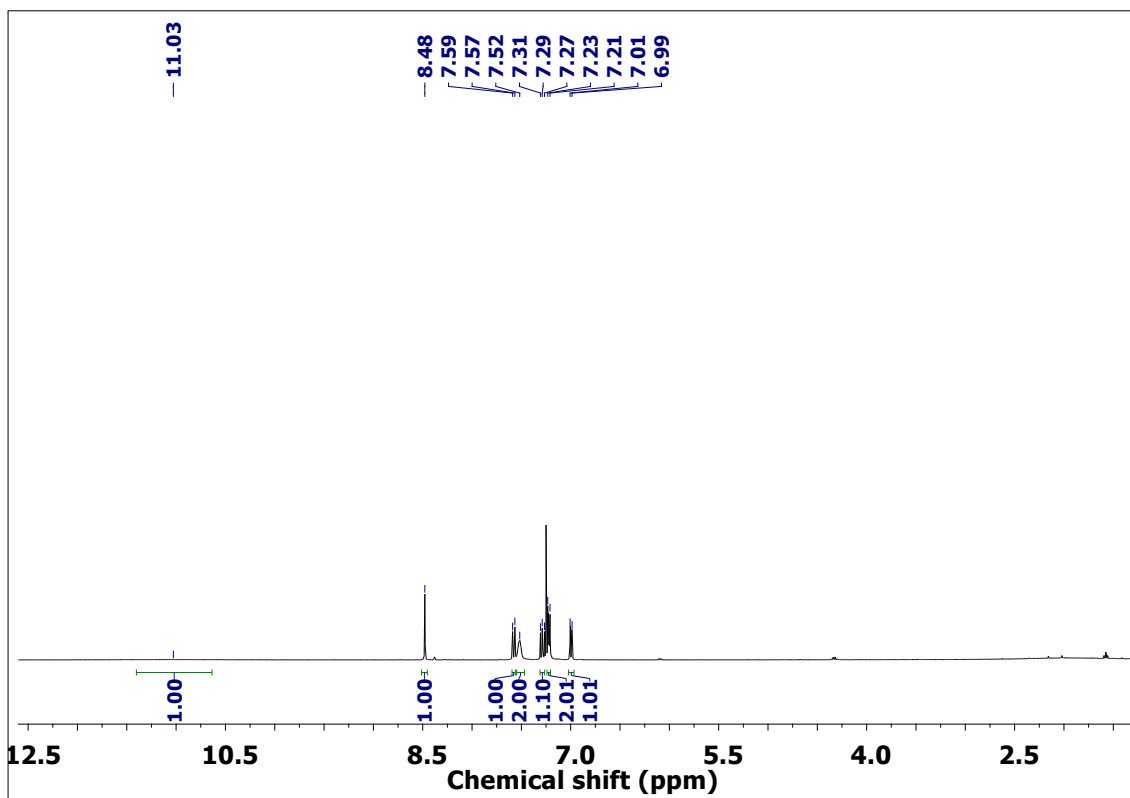


Figure S7.  $^{13}\text{C}$ NMR (100 MHz,  $\text{CDCl}_3$ ) of compound C2.

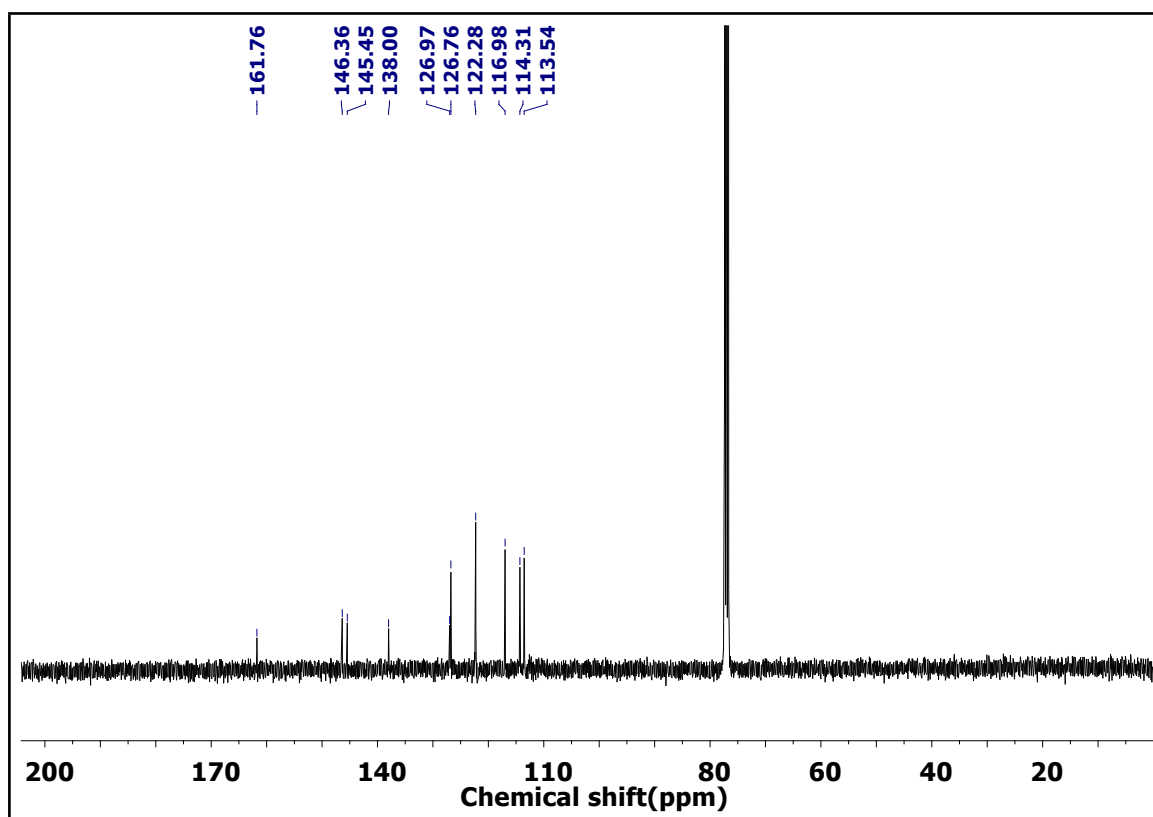
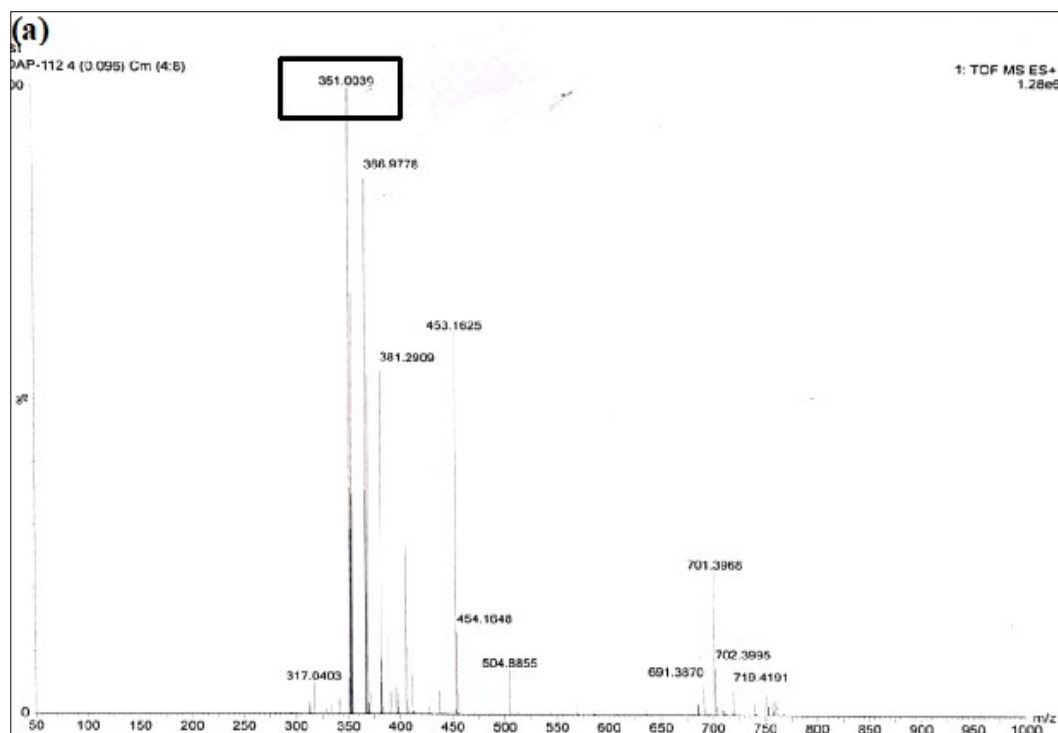
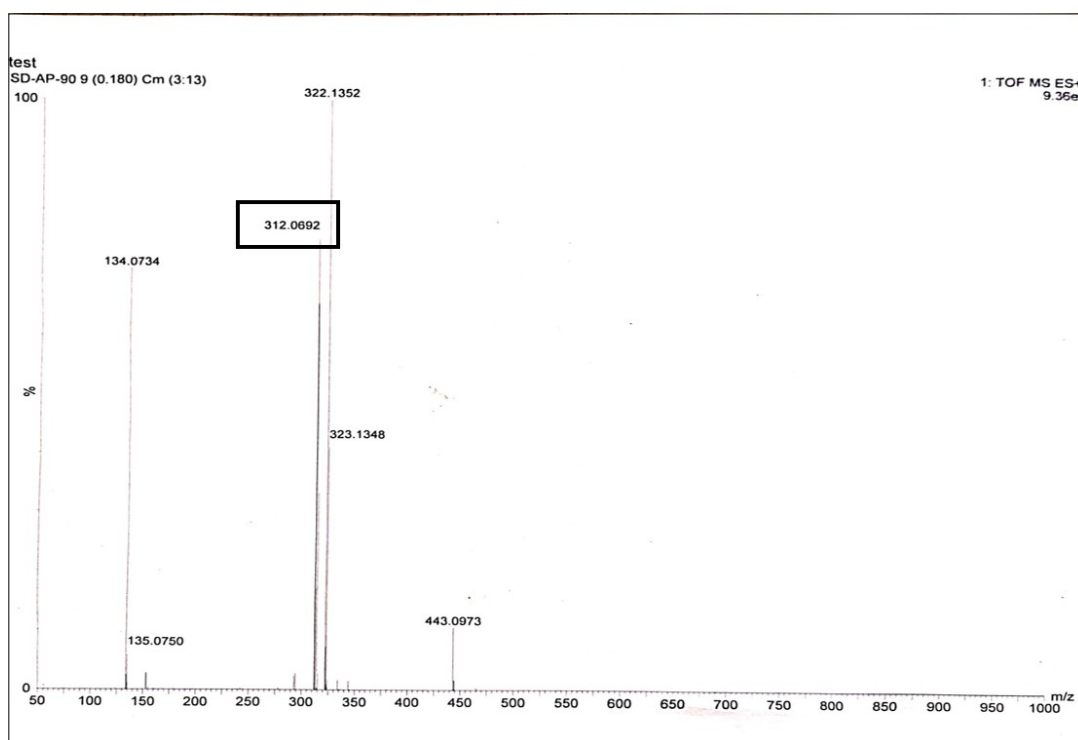


Figure S8. ESI-HRMS spectra of C1. The isotopic pattern at  $m/z=351.0039$  can be attributed to  $[\text{C1.Na}^+]$  ( $m/z_{\text{calculated}} = 351.0078$ ).



**Figure S9.** ESI-HRMS spectra of C2. The isotopic pattern at  $m/z= 312.0692$  can be attributed to  $[C_2.H^+]$  ( $m/z_{\text{calculated}} = 312.0647$ ).



### LOD, binding constant, and stoichiometry

Evaluating absorption and emission data collected after titration gives binding constant and limit of detection. Binding constant calculated by employing

$$\text{Intercept/slope} = \text{Binding constant}$$

Values obtained by linear fitting the importance of  $1/\Delta\epsilon$  vs.  $1/[F^-]$ .

LOD of compounds were obtained by placing the equation

$$2\sigma/\text{slope}$$

Here,  $\sigma$  stand for the stander deviation of the regression line and slope obtained by the emission intensity vs. concentration plot.

**Figure S10.** We are calibrating linear fit curve<sup>1</sup> of emission at 444nmof C1 (Acetonitrile) to obtain (a) Binding constant ( $3.24 \times 10^3$ ) and (b) LOD ( $1.45 \times 10^{-6}$ ).

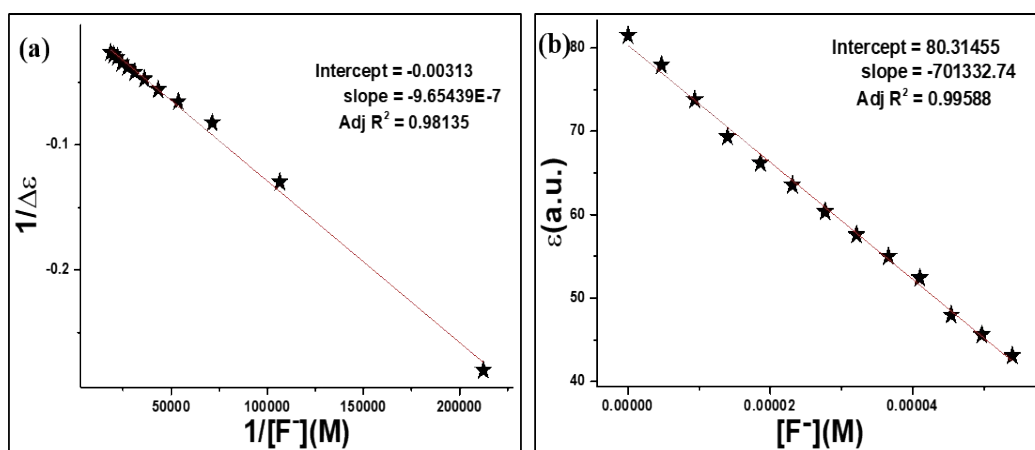


**Figure S11.** We are calibrating linear fit curve<sup>1</sup> of absorbance at 309nm of C1 (Acetonitrile) to obtain (a) Binding constant ( $1.55 \times 10^4$ ) and (b) LOD ( $2.46 \times 10^{-4}$ ).

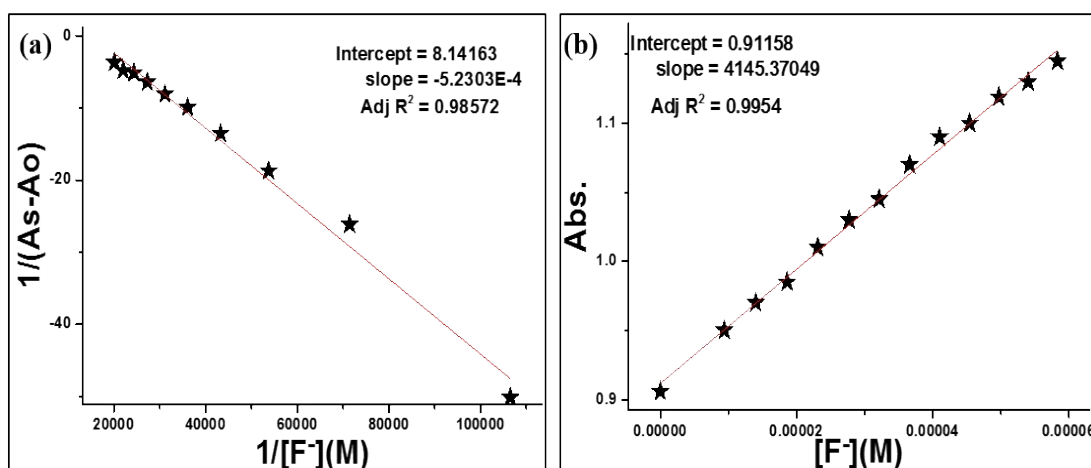


**Figure S12.** Calibrating linear fit curve<sup>1</sup> of emission at 422nm (water) of C2 to obtain (a) Binding constant ( $3.4 \times 10^3$ ), (b) LOD ( $9.8 \times 10^{-8}$ ).

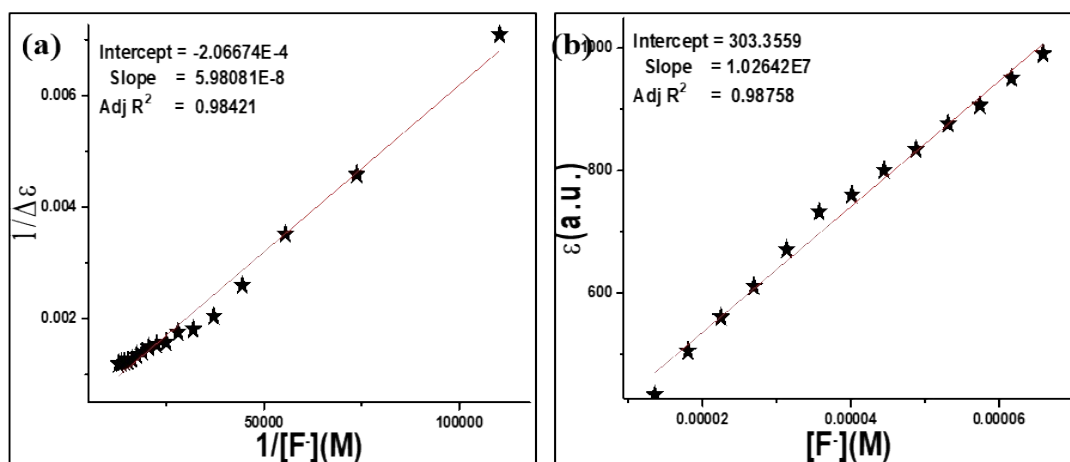
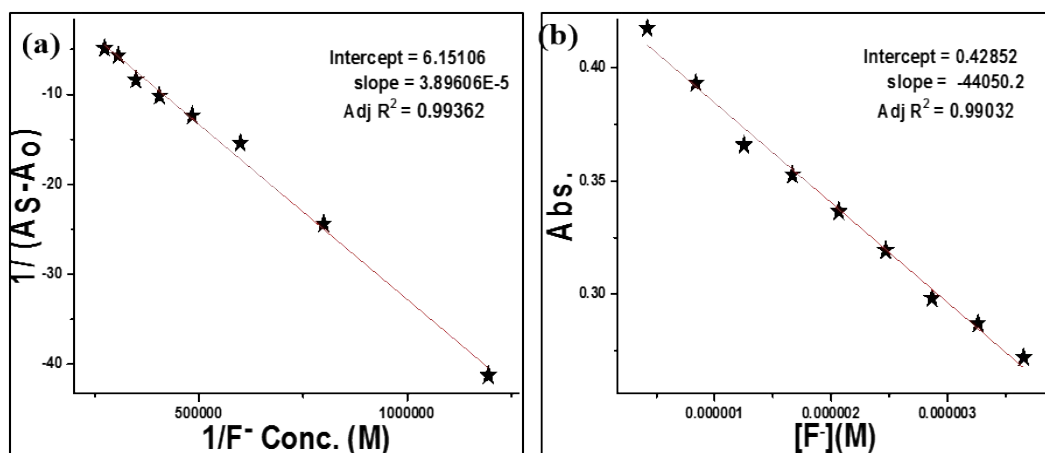


**Figure S13.** We are calibrating linear fit curve<sup>1</sup> of absorbance at 309nm of C2 to obtain (a) Binding constant ( $1.58 \times 10^5$ ) and (b) LOD ( $2.31 \times 10^{-5}$ ).



### Emission titration

**Figure S14.** Emission spectra of (a) C1 in different solvents (b) C1 in the presence of anions.

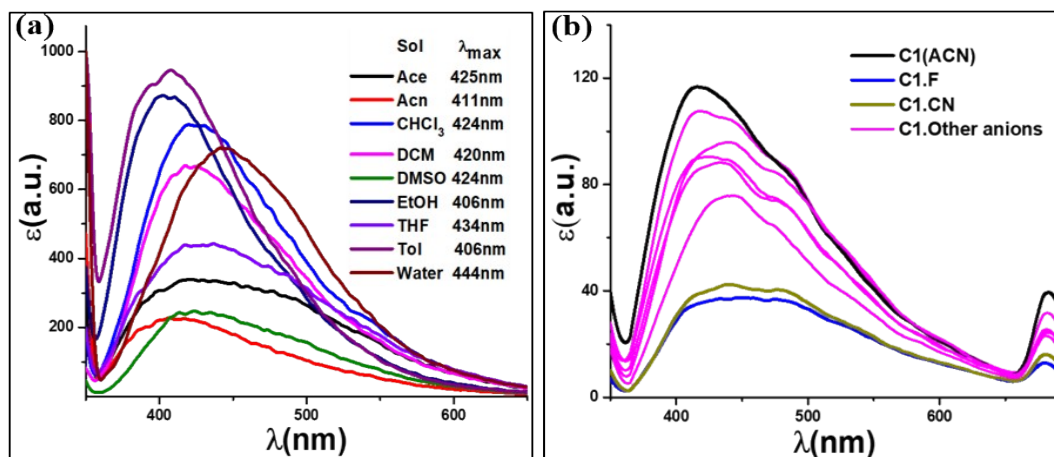


**Figure S15.** (a) Titration of C1 with  $F^-$  (b) Titration of C2 with  $F^-$  in acetonitrile. Emission spectra of C1.

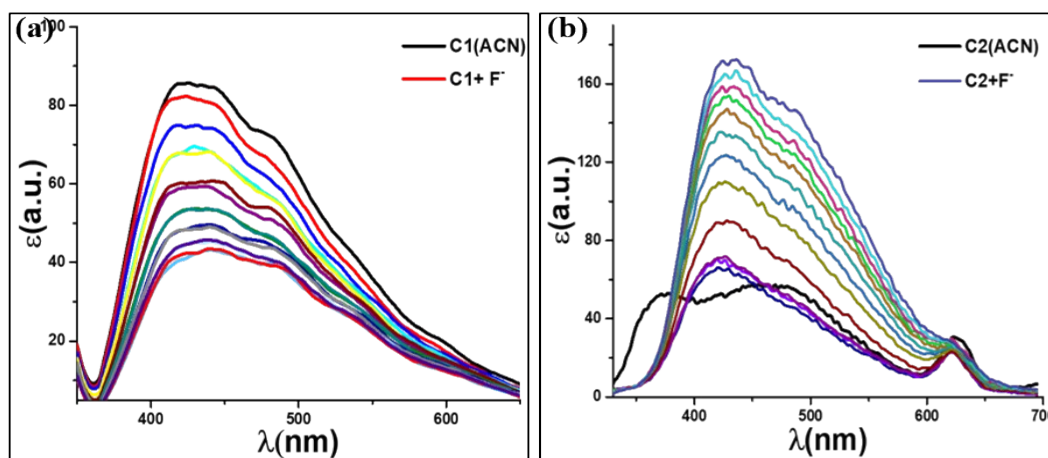


**Figure S16.** Depiction of change in absorbance of C1 and C2 with  $F^-$ .

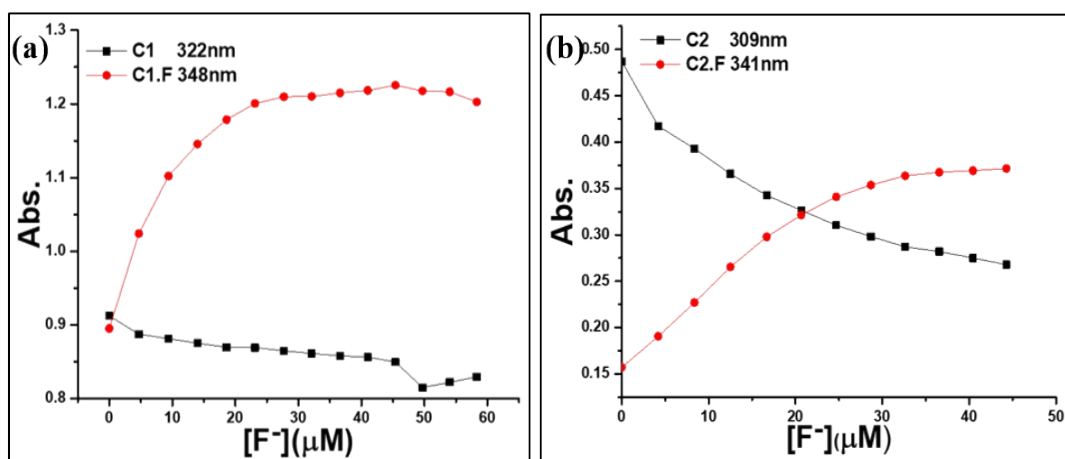
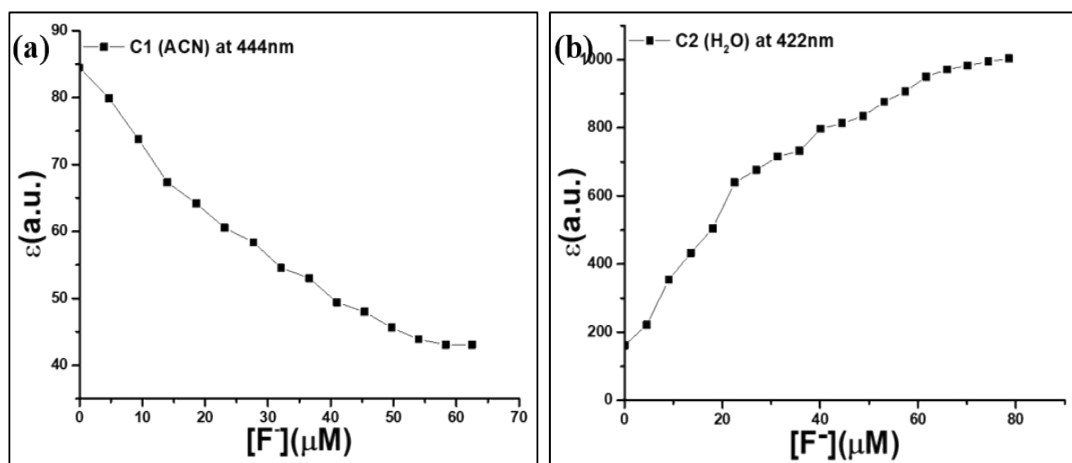
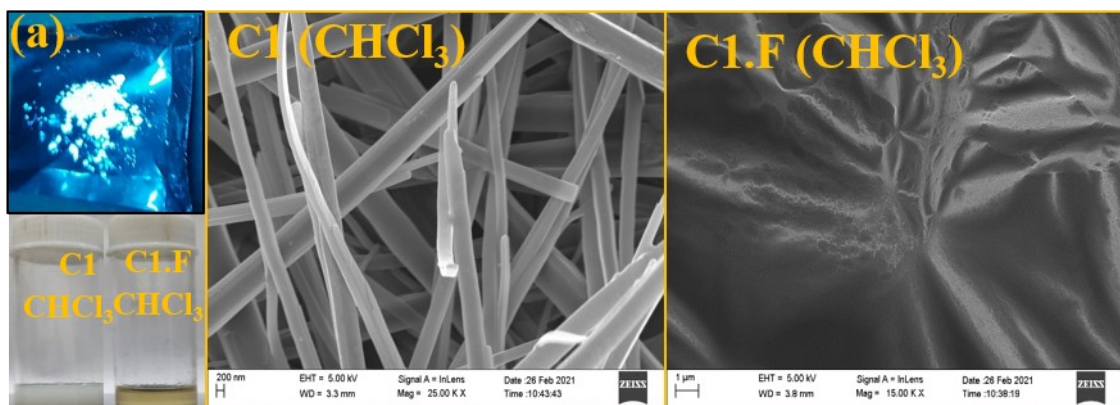


Figure S17. Depiction of change in emission intensity of C1 and C2 with  $F^-$ .



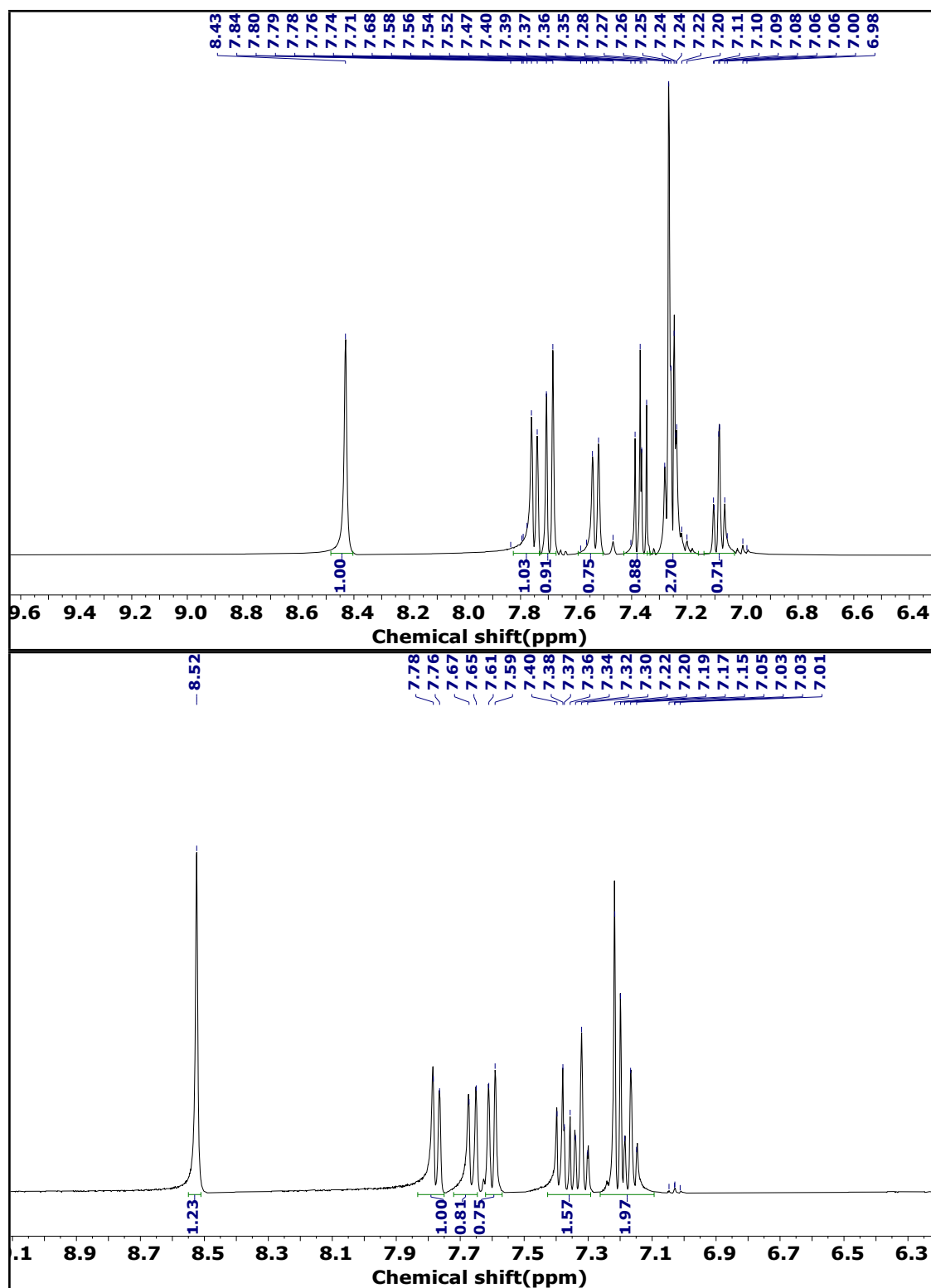
### Mysterious behavior of C1 in $\text{CHCl}_3$

Figure S18. (a) Image of C1 powder in exposure to long-range light (white fluorescence in nature). FE-SEM and solution phase image support this behavior of C1 in  $\text{CHCl}_3$ .

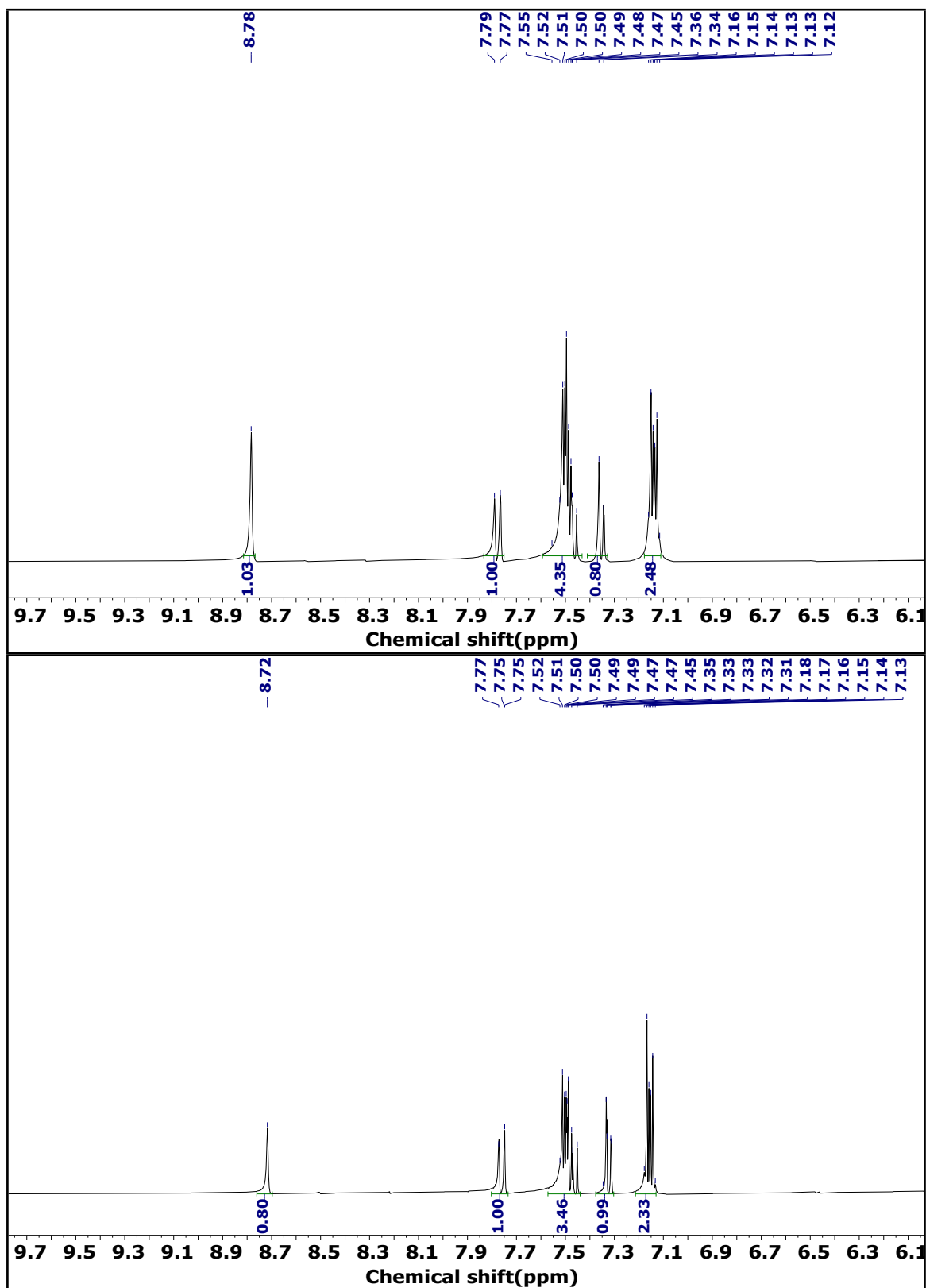


## D<sub>2</sub>O exchange of compounds in <sup>1</sup>H NMR

**Figure S19.** <sup>1</sup>H NMR (400MHz, DMSO) spectra of C1 (above) and C1 after D<sub>2</sub>O addition (below). The peak at 7.28ppm shows D<sub>2</sub>O exchange via reduced integration value.<sup>2</sup>



**Figure S20.**  $^1\text{H}$ NMR (400MHz, DMSO) spectra of C2 (above) and C2 after  $\text{D}_2\text{O}$  addition (below). The peak at 7.55ppm shows a  $\text{D}_2\text{O}$  exchange reaction.<sup>2</sup>



## $^1\text{H}$ and $^{19}\text{F}$ NMR spectra of complexes

**Figure S21.**  $^1\text{H}$ NMR(400 MHz,  $\text{CDCl}_3$ ) of (a)  $\text{C1.F}^-$  and (b)  $\text{C2.F}^-$  having 20eq of  $\text{F}^-$ , up to a range of 13 to 19 ppm.<sup>2,3</sup>

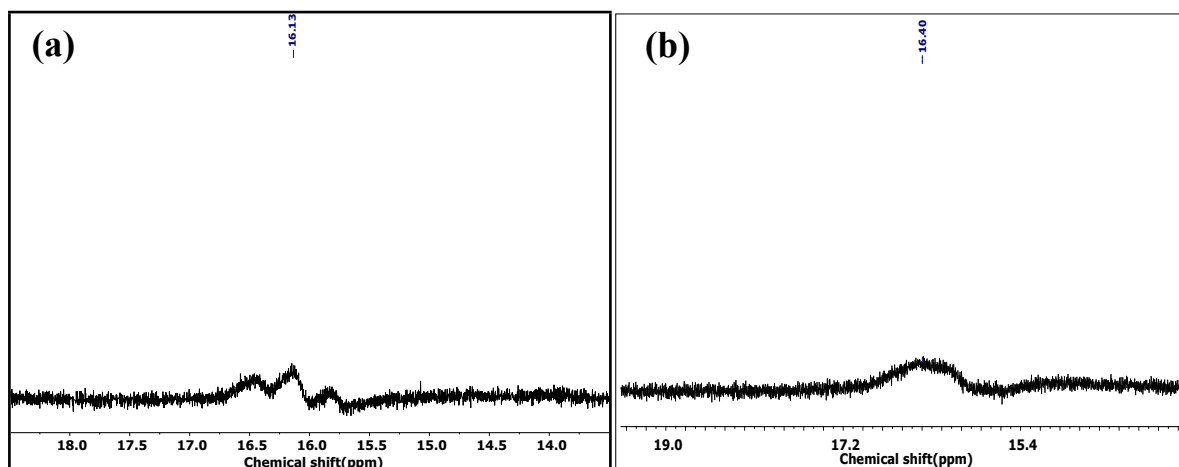


**Figure S22.**  $^{19}\text{F}$ NMR (377 MHz,  $\text{CDCl}_3$ ) spectra of  $\text{C1.F}^-$ . The desired triplet peak obtained at 144ppm signified that deprotonated fluoride ion  $[\text{H}_2.\text{F}]^-$ .<sup>3</sup>

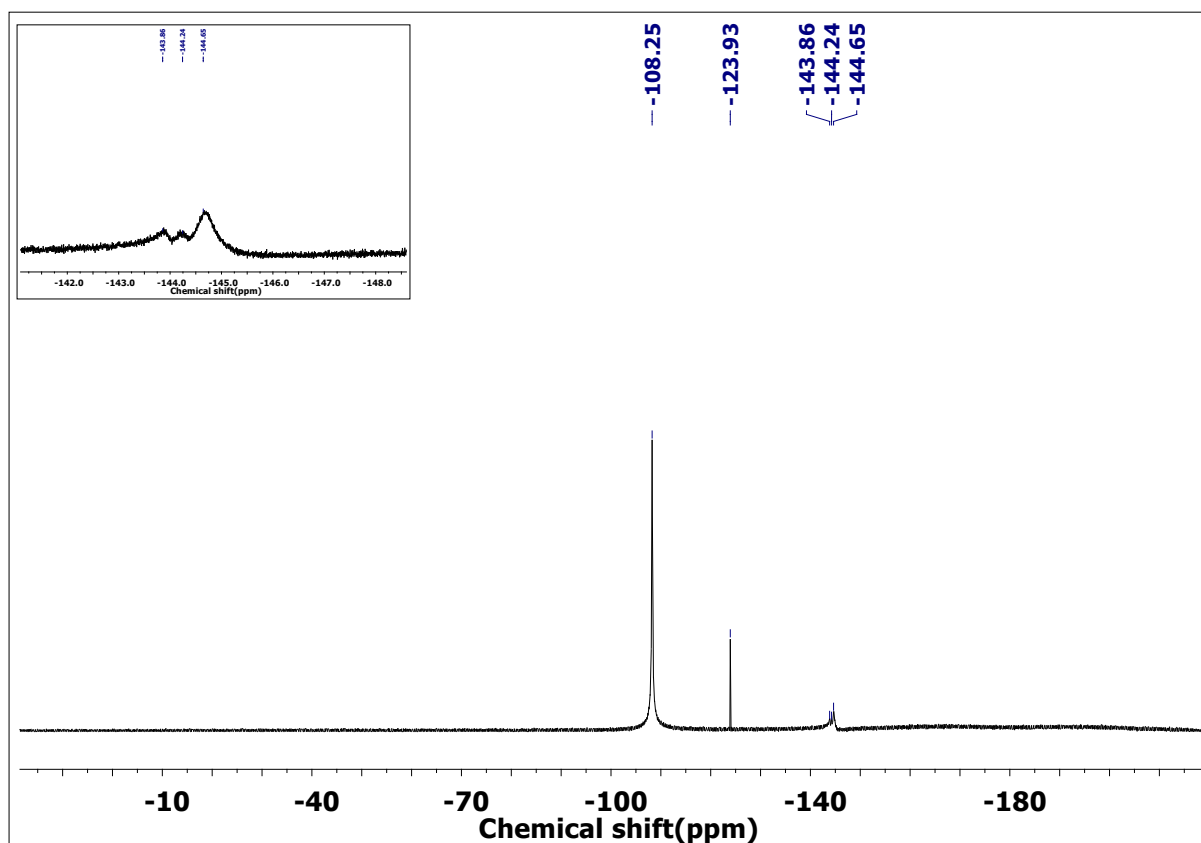


**Figure S23.**  $^{19}\text{F}$ NMR (377 MHz,  $\text{CDCl}_3$ ) spectra of  $\text{C}_2\text{F}^-$ . The desired peak between 130 to 170ppm obtained signified that deprotonated fluoride ion  $[\text{H}_2\text{F}^-]$  formed.<sup>3</sup>

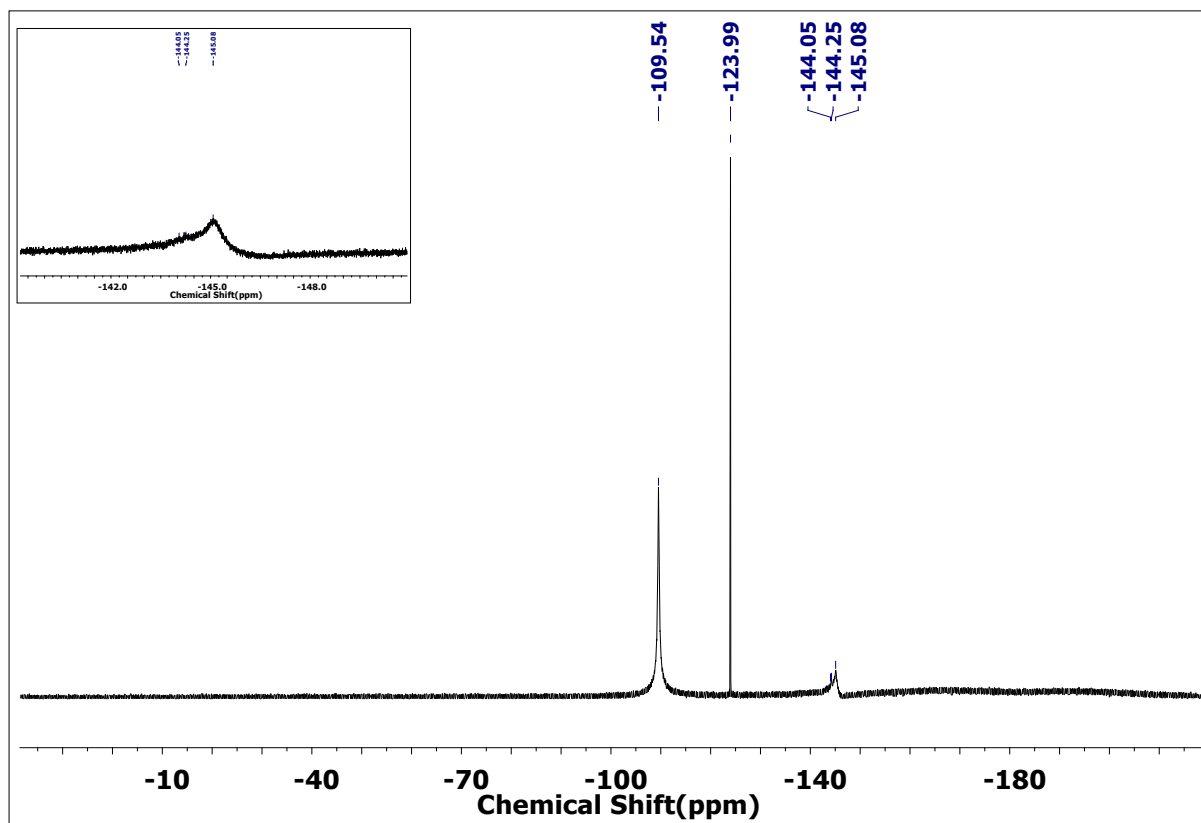


**Figure S24.**  $^{19}\text{F}$ NMR (377 MHz,  $\text{CDCl}_3$ ) spectra of  $\text{TBAF}^-$ . The desired peak was obtained at 124.62ppm.

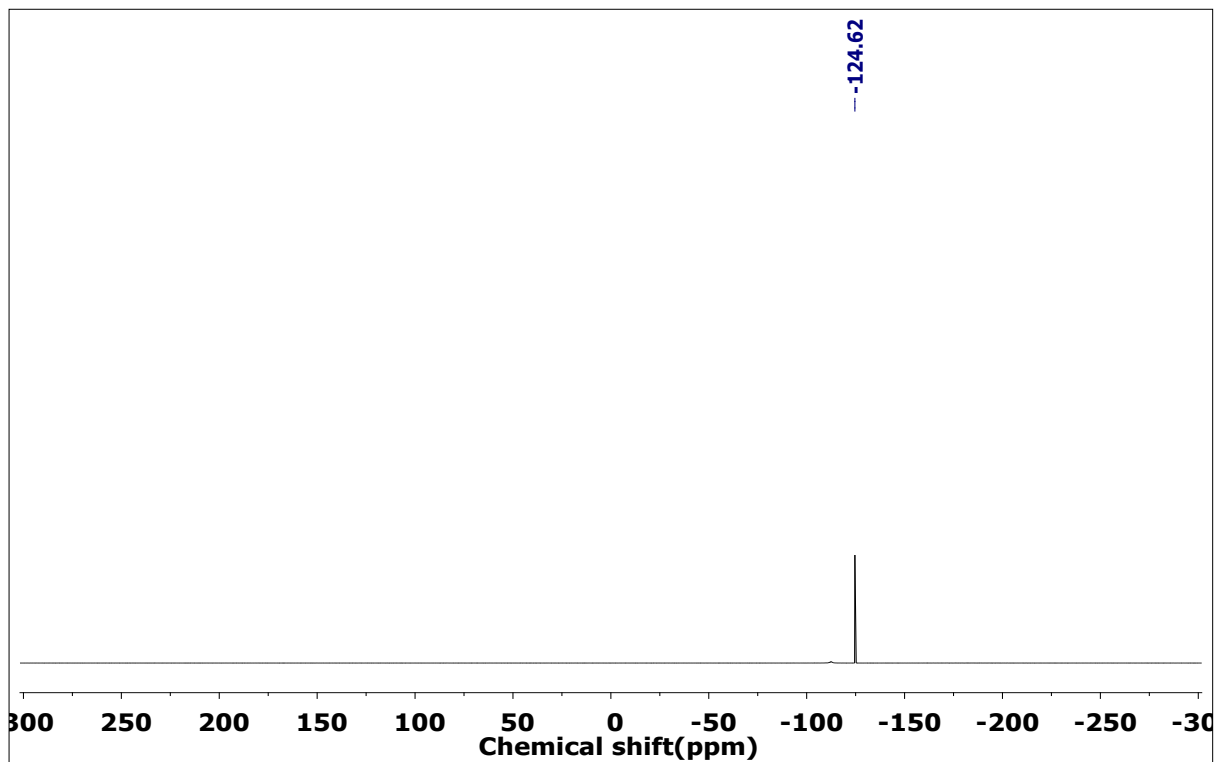
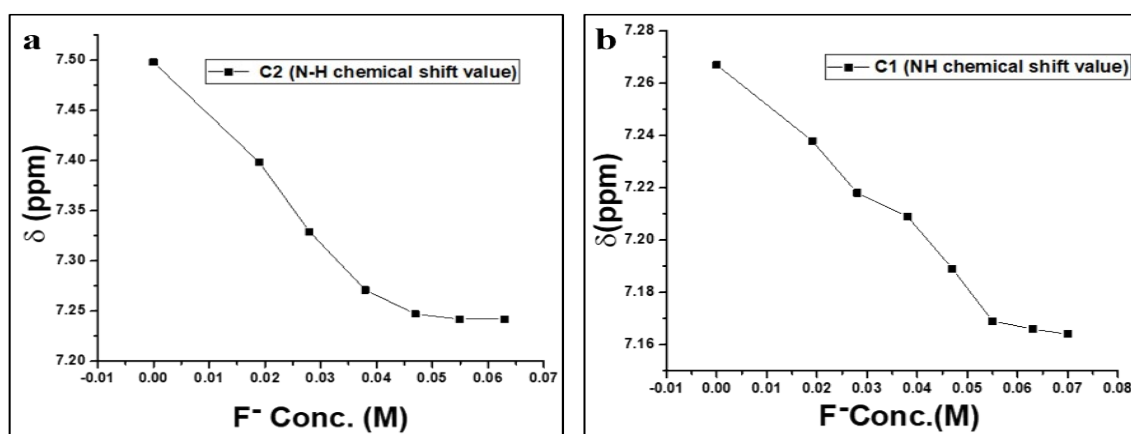
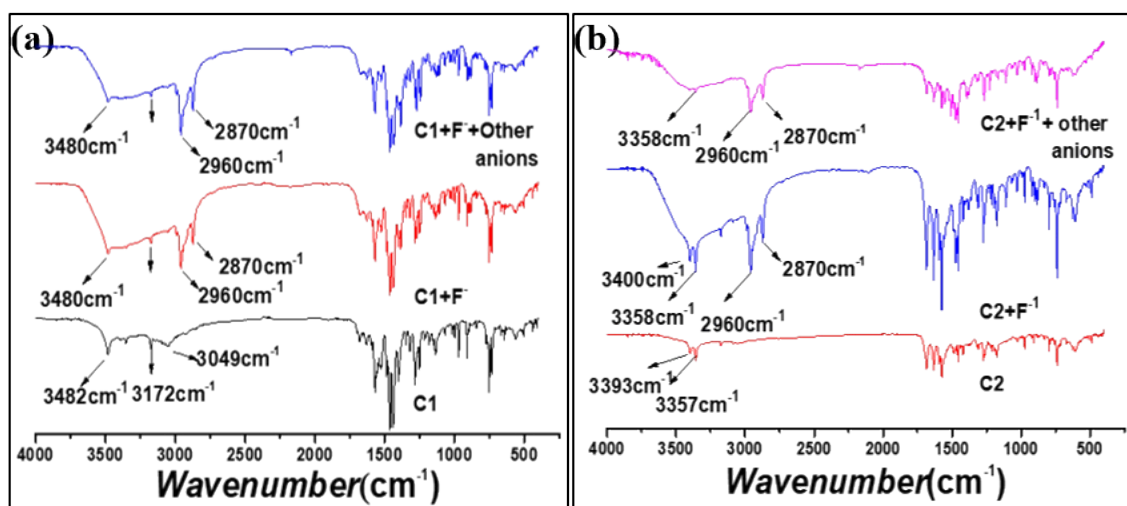


**Figure S25.** Fluoride anion concentration added versus chemical shift value of (a) C1 and (b) C2.



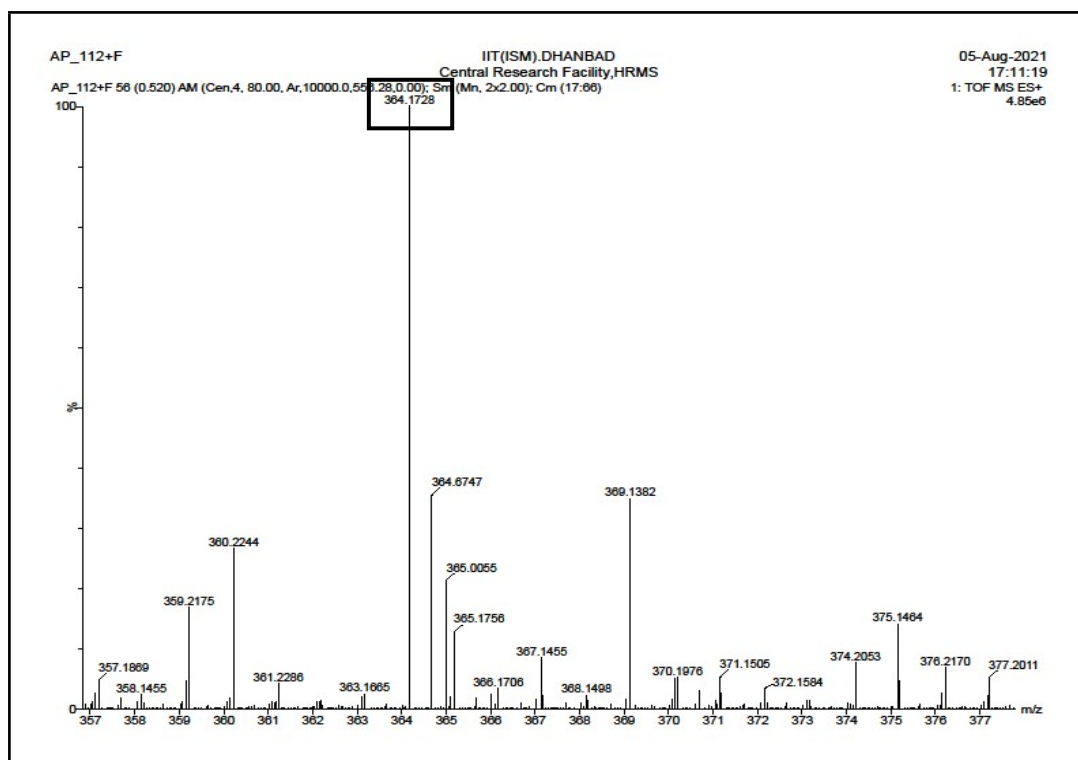
### FT-IR spectroscopy

**Figure S26.** FT-IR plots of (a) C1 and (b) C2.

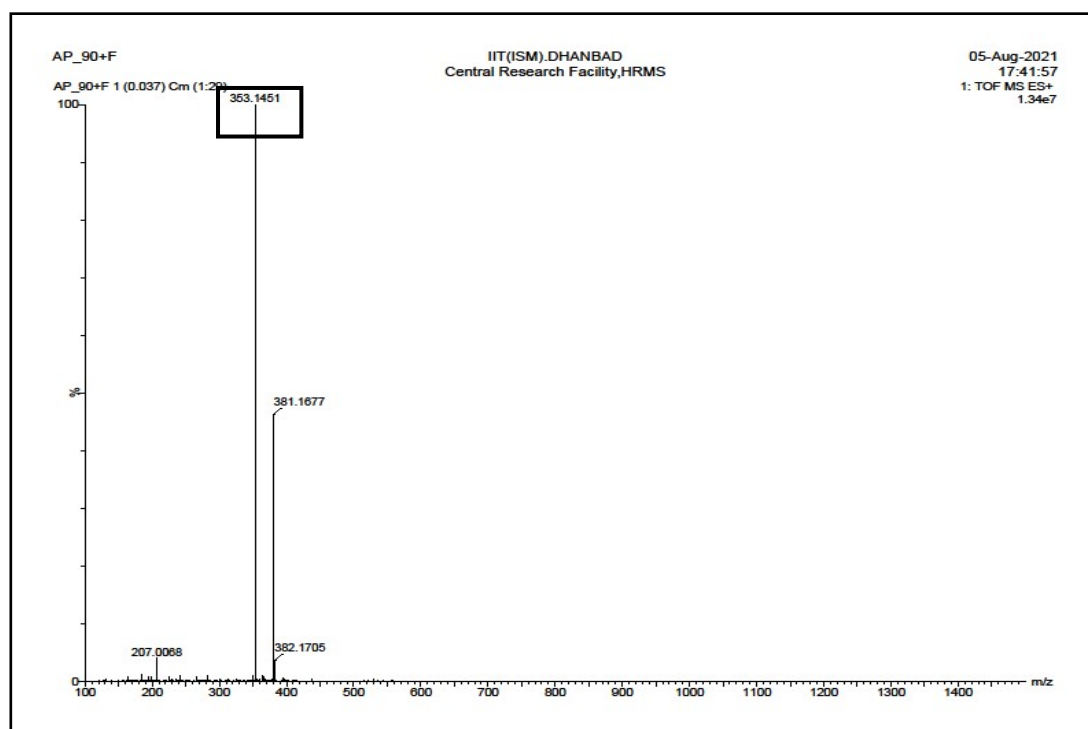


### HR-MS spectrum of complexes

**Figure S27.** ESI-HRMS spectra of C1.S (m/z calculated for [C1+F+H<sub>2</sub>O-H] = 364.0203 and obtained 364.1728)

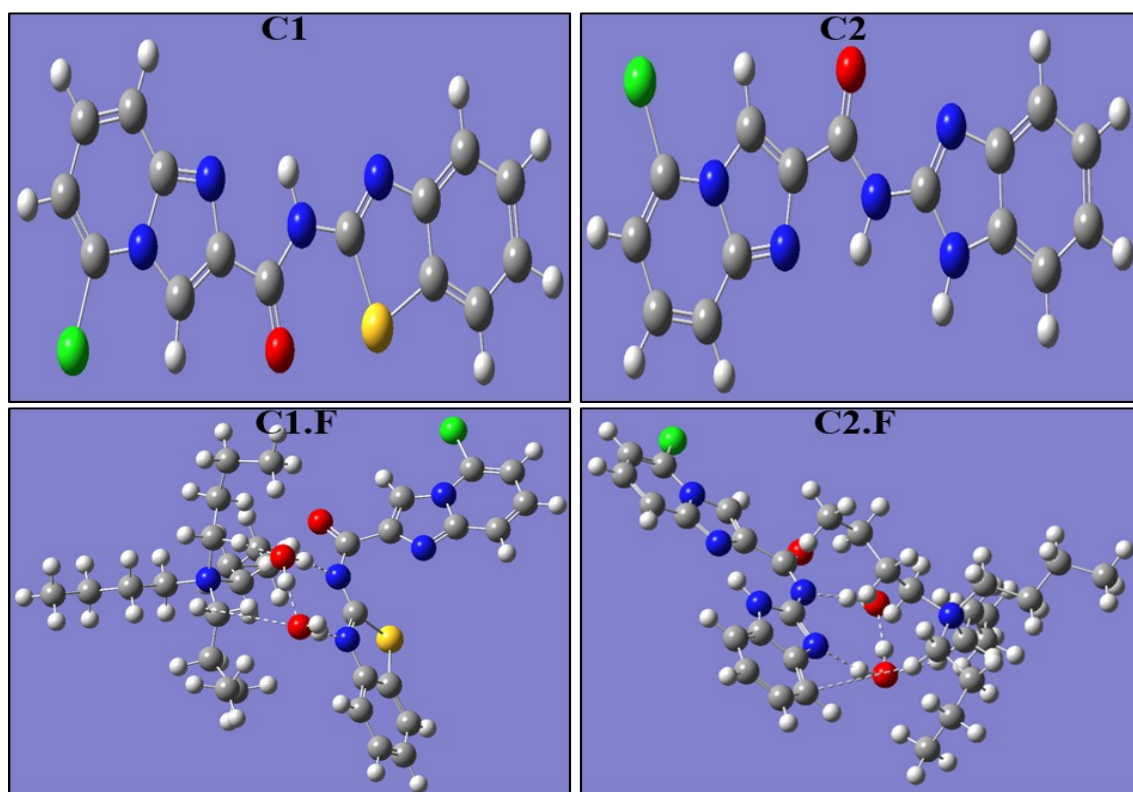


**FigureS28.** ESI-HRMS spectra of **C2.S** ( $m/z$  calculated for  $[C1+F+Na] = 353.0461$  and obtained 353.1451).



### DFT calculated optimized structure

**Figure S29.** DFT optimized C1, C2, C1.S, and C2.S using B3LYP /3-21G basis set on the Gaussian09 program.



### Titration plot of carboxamide with CN<sup>-</sup>

**Figure S30.** Absorption titration spectra of (a) C1 and (b) C2 with CN<sup>-</sup>.

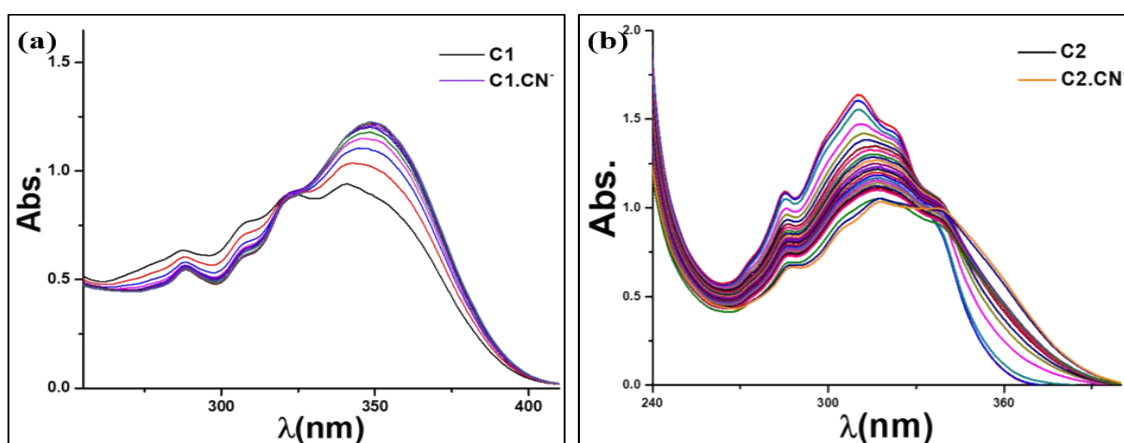


**Figure S31.** <sup>1</sup>H NMR titration profile of C1 with cyanide anion.

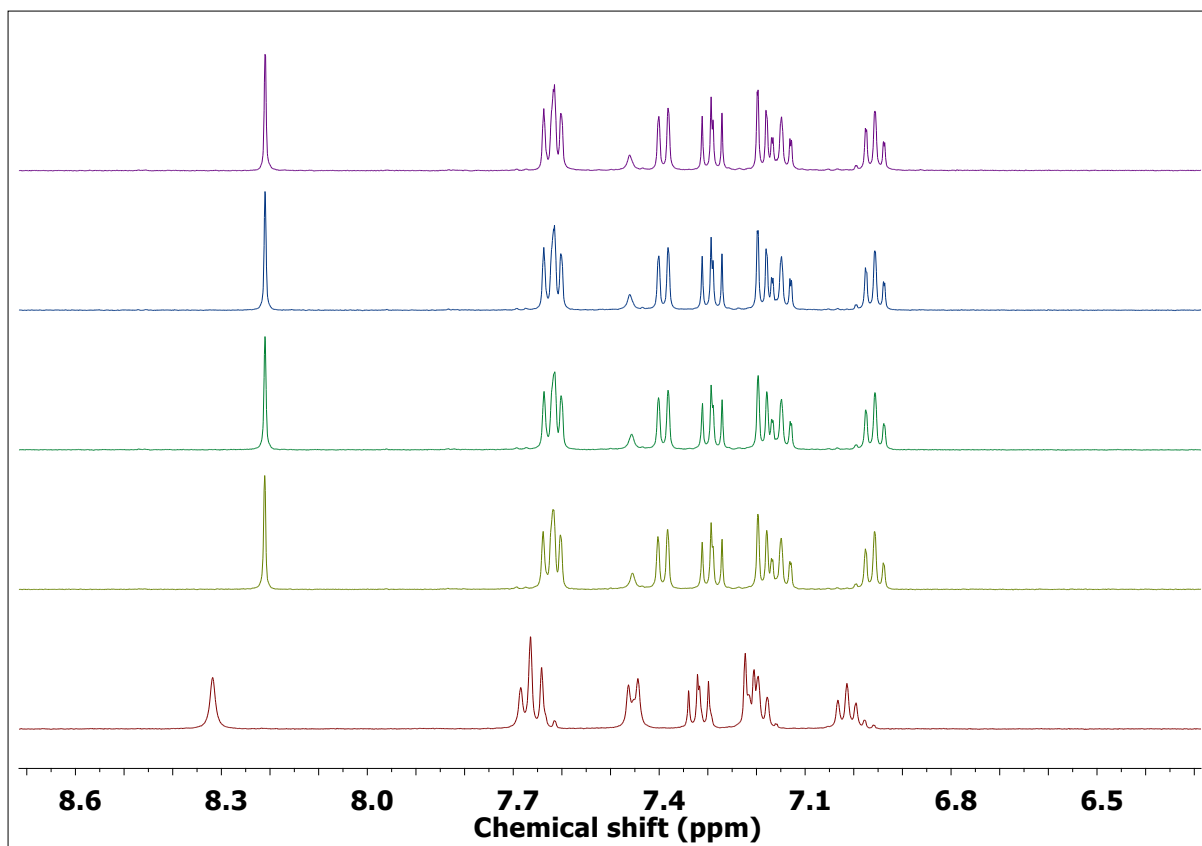
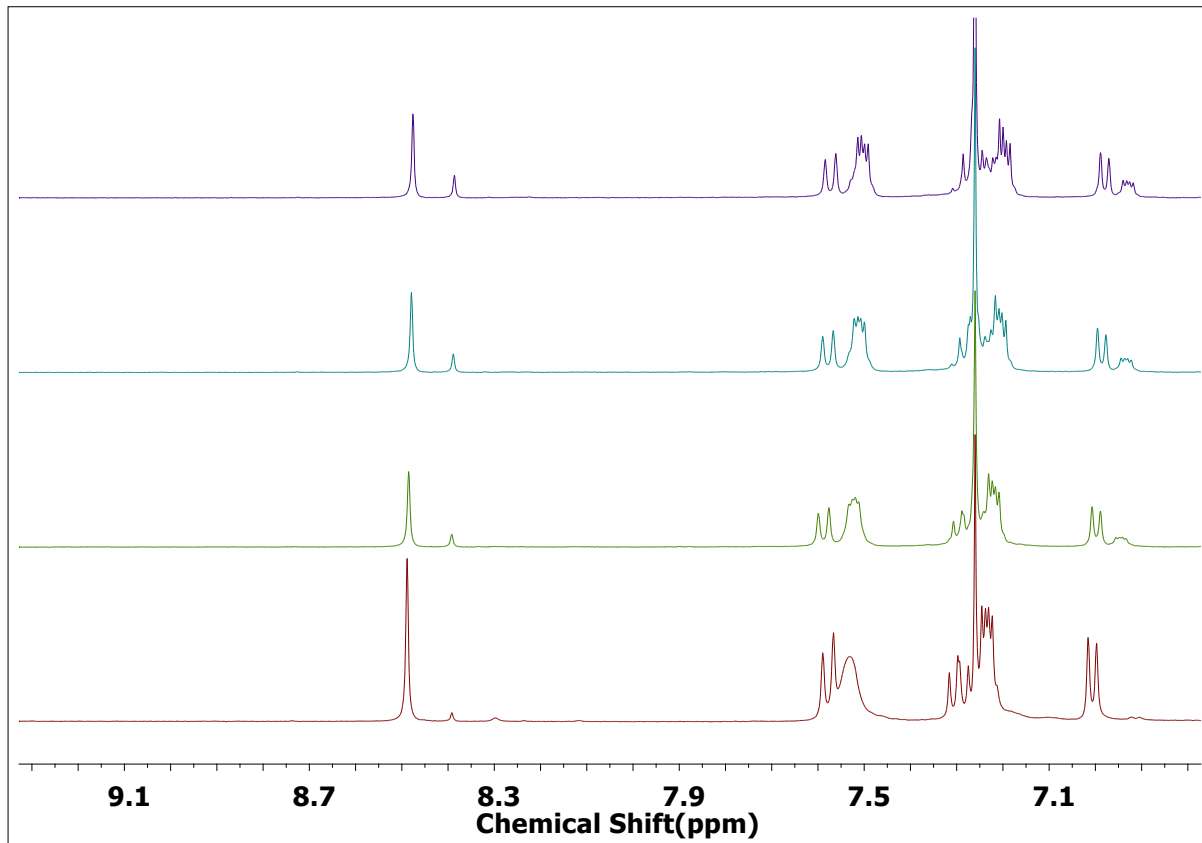
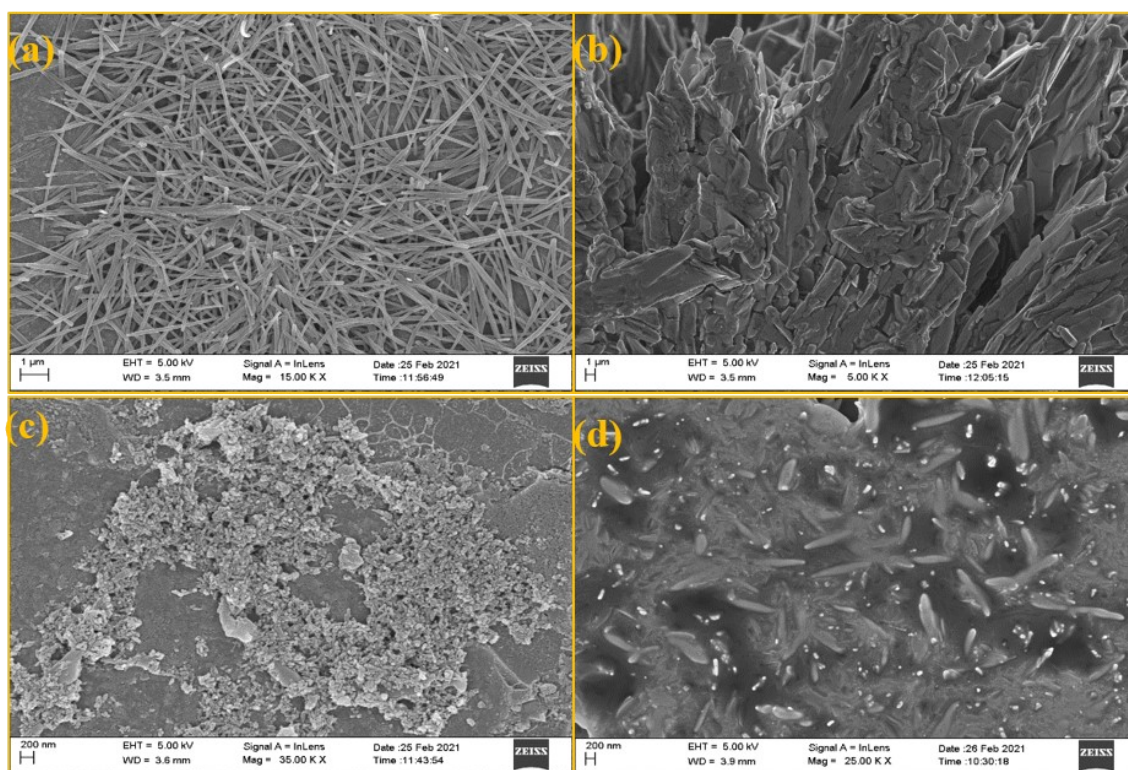


**Figure S32.**  $^1\text{H}$ NMR titration profile of C2 with cyanide anion.



## FE-SEM image

**Figure S33** FESAM image of (a) C1,(b) C1.S,(c) C2,and (d) C2.S. Sample prepared in DMSO for C1 and C1.S and in water for C2 and C2.S through drop caste method.



## References

1. (a) J. Wu, G. Lai, Z. Li, Y. Lu, T. Leng, Y. Shen and C. Wang, *Dye. Pigment.*, 2016, **124**, 268–276. (b) N. Kaur and G. Jindal, *Spectrochim. Acta - Part A Mol. Biomol. Spectrosc.*, 2019, **223**, 1–7.
2. N. Luo, J. Li, T. Sun, S. Wan, P. Li, N. Wu, Y. Yan and X. Bao, *RSC Adv.*, 2021, **11**, 10203–10211.
3. (a) H. J. Han, J. H. Oh, J. L. Sessler and S. K. Kim, *Chem. Commun.*, 2019, **55**, 10876–10879. (b) M. Goursaud, P. De Bernardin, A. Dalla Cort, K. Bartik and G. Bruylants, *European J. Org. Chem.*, 2012, **2012**, 3570–3574.